Liquid Marble Interaction Gate for Collision-Based Computing

Thomas C. Draper[a], Claire Fullarton[a], Neil Phillips[a], Ben P. J. de Lacy Costello[b], Andrew Adamatzky[a,*]

[a] *Unconventional Computing Laboratory, University of the West of England, Bristol, United Kingdom*
[b] *Institute of Biosensing Technology, Centre for Research in Biosciences, University of the West of England, Bristol, United Kingdom*

Abstract

Liquid marbles are microlitre droplets of liquid, encapsulated by self-organised hydrophobic particles at the liquid/air interface. They offer an efficient approach for manipulating liquid droplets and compartmentalising reactions in droplets. Digital fluidic devices employing liquid marbles might benefit from having embedded computing circuits without electronics and moving mechanical parts (apart from the marbles). We present an experimental implementation of a collision gate with liquid marbles. Mechanics of the gate follows principles of Margolus' soft-sphere collision gate. Boolean values of the inputs are given by the absence (FALSE) or presence (TRUE) of a liquid marble. There are three outputs: two outputs are trajectories of undisturbed marbles (they only report TRUE when just one marble is present at one of the inputs), one output is represented by trajectories of colliding marbles (when two marbles collide they lose their horizontal momentum and fall), this output reports TRUE only when two marbles are present at inputs. Thus the gate implements AND and AND-NOT logical functions. We speculate that by merging trajectories representing AND-NOT output into a single channel one can produce a one-bit half-adder. Potential design of a one-bit full-adder is discussed, and the synthesis of both a pure nickel metal and hybrid nickel/polymer liquid marble is reported.

Keywords: Liquid marble, Unconventional computing, Collision computing, Adder, Logic gate, Microfluidic

1. Introduction

Since their inception in 2001 [1], liquid marbles (LMs) have been a source of growing interest across fields as diverse as medicine [2, 3], engineering [4, 5]

*Corresponding author
Email address: Andrew.Adamatzky@uwe.ac.uk (Andrew Adamatzky)

and chemistry [6, 7]. LMs are constructed from microlitre droplets of water, supported by a layer of hydrophobic particles on the surface. In this manner, the hydrophobic particles minimise the comparatively high surface energy of water by encapsulating the droplet, and keeping it near spherical. This permits the water droplet to remain non-wetting on many (traditionally wettable) surfaces.

There are two major variables affecting the properties of a LM: the core and the coating. Traditionally the encapsulated liquid is water, although there are a range of both common (glycerol [1]) and uncommon (petroleum [8]) alternatives. The coating provides the largest affect on the mechanical properties of the marble, as it is the coating that interacts with the surface the LM is resting on. Coating parameters that can be modified to impart the desired properties include the composition, grain size, and mix ratio. By varying these, it is possible to adapt a liquid marble to many different situations.

Liquid marbles have previously been investigated as fluidic transport devices. They are ideally suited to the transport of microlitre quantities of liquid, due to their non-wetting nature. Recent progress have been made in this area, with LM movement initiated by magnets [9], electrostatic fields [10], gravity [1], lasers [6] and the Marangoni effect [11] all reported. The movement of LMs can be exploited for chemical reactions, by controlling the time and place of reagent mixing. This has been demonstrated both with the coalescing of LMs [12], and in the controlled destruction of LMs once they arrive at a chosen location [13, 14].

In interaction gates, Boolean values of inputs and outputs are represented by presence of physical objects at given site at a given time. If an object is present at input/output we assume that logical value of the input/output is TRUE; if the object is absent the logical value is FALSE. The signal-object realise a logical function when they pass through a collision site. The objects might fuse, annihilate or deflect on impact.

The fusion gate (figure 1(a)) was first implemented in fluidic devices in the 1960s. The gate is the most well known (on a par with the bistable amplifier) device in fluidics [15, 16]: two nozzles are placed at right angles to each other, when there are jet flows in both nozzle they collide and merge into a single jet entering the central outlet. If the jet flow is present only in one of the input nozzles it goes into the vent. The central outlet represents AND and the vent represent AND-NOT. The fusion-based gate was also employed in designs of computing circuits in Belousov-Zhabotinsky medium [17–20], where excitation wave-fragments merge when collide; in the actions of slime mould [21], when distributing vesicles collide; and a crab-based gate [22], were swarms of solider crabs merge into a single swarm.

In the annihilation gate (figure 1(b)) signals disappear on impact. This gates has two-inputs and two-outputs, each of the outputs represents AND-NOT. Computational universality of the Conway's Game of Life cellular automata was demonstrated using annihilation based collisions between gliders [23]. We can also implement the annihilation gate by colliding excitation wave-fragments at certain angles [24].

Key deficiency of the fusion and annihilation gates is that, when implemented

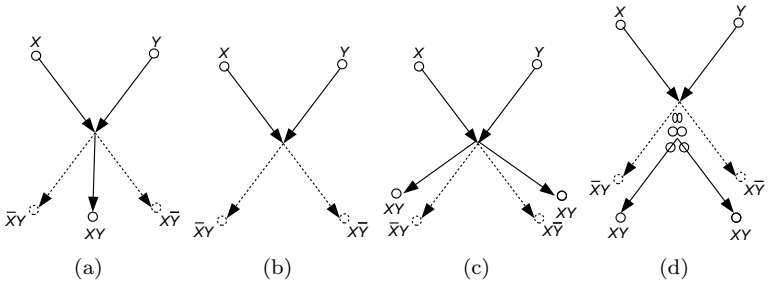

Figure 1: Interaction-based gates. (a) Fusion of signals. (b) Annihilation of signals. (c) Elastic deflection of signals. (d) Quasi-elastic deflection of compressible signals.

in media other than excitable spatially-extended systems, they do not preserve physical quantity of signals, e.g. when two signals merge the output signal will have a double mass of a signal input signal. This deficiency is overcome in the conservative logic, proposed by Fredkin and Toffoli in 1978 [25]. The logical value are represented by solid elastic bodies, aka billiard balls, which deflect when made to collide with one another (figure 1(c)). Intact output trajectories of the balls represent AND-NOT function, output trajectories of deflected balls represent AND function. The gates based on elastic collision led to development of a reversible (both logically and physically) gate: Fredkin [25] and Toffoli [26] gates, which are the key elements of low-power computing circuits [27, 28], and amongst the key components of quantum [29–32] and optical [33] computing circuits.

The soft-sphere collision gate proposed by Margolus [34] gives us a rather realistic representation of interaction gates with real-life physical and biological bodies, interacting in a quasi-elastic compressible manner (figure 1(d)). Logical value $x = 1$ is given by a ball presented in input trajectory marked x, and $x = 0$ by the absence of the ball in the input trajectory x; the same applies to $y = 1$ and $y = 0$, respectively. When the two balls, approaching the collision gate along paths x and y collide, they compress but then spring back and reflect. As a result, the balls come out along the paths marked xy. If only one ball approaches the gate, that is for inputs $x = 1$ and $y = 0$ or $x = 0$ and $y = 1$, the balls exit the gate via path $x\overline{y}$ (for input $x = 1$ and $y = 0$) or $\overline{x}y$ (for input $x = 0$ and $y = 1$). Soft-sphere-like gates have been implemented using microlitre sized water droplets on a superhydrophobic copper surface [35]. Using channels cut into the surface, NOT-FANOUT, AND-OR and FLIP-FLOP gates were demonstrated. The water droplets only rebounded in a very narrow collision property window, and a thorough & complete superhydrophobic surface treatment was required.

In this paper, we report the first exploitation of liquid marbles for implementation of interaction gates. The gate realised in the experimental laboratory conditions is a combination of the fusion and the Margolus gate: output trajectories of collided liquid marbles are so close that they can be interpreted as a single output. That said, if required, two liquid marbles at the output can

be diverted along different paths to conserve a number of signals. By taking advantage of the liquid marbles' inherently low hysteresis, high tunability and capacity for enhanced versatility, we demonstrate the first step toward liquid marble facilitated, collision-based computing.

2. Materials & Method

2.1. Regular & Reliable Liquid Marble Formation

We first developed a technique for the regular and automatic formation of invariable LMs. This was achieved by programming a syringe driver (CareFusion Alaris GH) to feed a 21 gauge needle (0.8 mm diameter) at a typical rate of $7.0\,\mathrm{ml\,h^{-1}}$. The rate can be easily increased or decreased, and this rate gave sufficiently fast LM formation for our purpose. The produced droplets ($11.60 \pm 0.16\,\mu\mathrm{l}$) were permitted to fall onto a sheet of acrylic, slanted to 20° from horizontal, and surface-treated with a commercial hydrophobic spray (Rust-Oleum® NeverWet®). This formed beads of water, which were allowed to roll over a bed of appropriate hydrophobic powder. The result was a continuous 'stream' of LMs with the same volume, coating and coating thickness. It should be noted that whilst the forming of LMs by running droplets down a powder slope has been separately developed by another group [14], our system prevents premature destruction of the powder bed by initially preforming the droplet on a treated hydrophobic surface.

2.2. Maintaining Timing for Collisions

In collision based computing, accurate timing is essential. As signals propagate through the system they must remain in sync, or the operation of many logic gates fails. In order to address this, an innovative system of electromagnets (EMs) was implemented. This was possible due to the generation of novel LMs with a mix of ultra-high density polyethylene (UHDPE) (Sigma-Aldrich, $3\text{–}6 \times 10^6\ \mathrm{g\,mol^{-1}}$, grain size approximately 100 µm) and nickel (GoodFellow Metals, 99.8 %, grain size 4 µm to 7 µm). A typical Ni/UHDPE coating was 2.5 mg. The use of UHDPE provides strength and durability, and the inclusion of ferromagnetic nickel allows for a versatile magnetic LM.

By positioning an electromagnet (100 N, 12.0 V DC, $29\,\mathrm{mm} \times 22\,\mathrm{mm}$) behind the acrylic slope, the rolling LM can be captured and released at will, by the switching on and off of said electromagnet. By controlling multiple, spatially-isolated electromagnets in series, non-concurrent LMs can be easily synchronised. To our knowledge, this is the first time electromagnets have been used to provide timing control with liquid marbles.

2.3. Gate Design for Liquid Marble Collisions

The collision gate was designed to allow for the colliding LMs to have a free path post-collision. This enabled the monitoring of the LM paths, and the future design and implementation of exiting pathways, creating a logic gate.

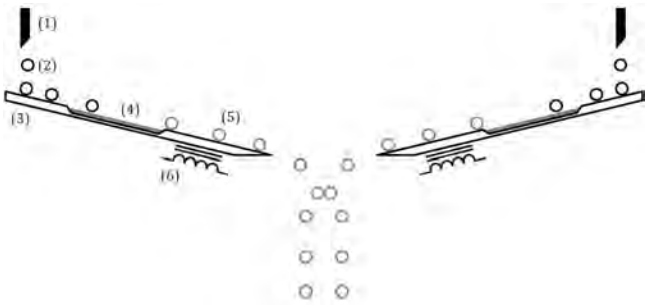

Figure 2: Schematic of our LM collider. Labelled numbers are: (1) syringe needle, (2) uncoated water droplet, (3) acrylic ramp, (4) hydrophobic powder bed, (5) liquid marble, and (6) electromagnet. Droplets form and fall out of the two syringe needles, landing on a superhydrophobic surface. They then roll over a bed of Ni/UHDPE powder, before being stopped and held stationary by the electromagnets. These electromagnets are then deactivated simultaneously, allowing the LMs to roll off and collide.

Two 16.0 cm acrylic pathways were slanted towards each other at 20°, affixed to an acrylic base sheet (3.0 mm thick). The acrylic base sheet was then aligned with a pitch of 38° from horizontal, giving a final LM pathway slope of 16° from the horizontal plane. This gave reliable LM rolling without extreme angles. The gap between the two slanted pathways was set at 1.6 cm, after empirical testing. A 2.0 cm, length at the top of each pathway was made hydrophobic, as discussed above. Parallel auto-formation of hybrid LMs was achieved using the syringe driver, delivering 11.6 µl of water per syringe per drop. Each droplet of water was permitted to land on the treated section of each slope, before rolling across the powder beds of UHDPE and Ni to form LMs. The two rolling LMs were then captured using the electromagnets, allowing for any slight timing deviations to be accounted for. On controlled synchronous (or asynchronous) release of the electromagnets, the LMs simultaneously roll off the acrylic ramps on collision trajectories. Collisions were recorded at 120 fps using a Nikon Coolpix P900, and played back frame-by-frame for analysis. A schematic of our LM collider can be seen in figure 2, and photographs of our LM collider can be seen in figure 3.

3. Discussion

3.1. Liquid Marble Lifetime

For a LM to be useful in a computing device, it has to have an appreciable lifetime. This is problematic for water based LM, as the gas permeability of LMs has previously been both established and exploited [5, 36–38]. As such, lifetime experiments were conducted on UHDPE LMs, Ni LMs, water droplets, and our new Ni/UHDPE hybrid LMs. Evaporation studies were conducted under ambient conditions, using 10.0 µl of DI water, and repeated seven times for each LM coating. UHDPE LMs were generated by rolling a droplet of water on a

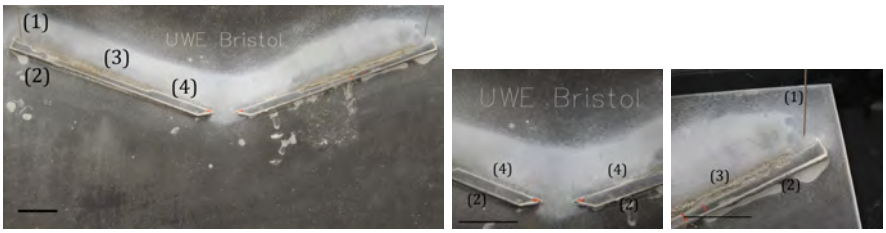

(a) (b) (c)

Figure 3: Photographs of our LM collider, showing (a) the overall layout, (b) an upclose of the magnetic breaking/release area, and (c) an upclose of the droplet formation area. Labels are: (1) syringe needle, (2) acrylic ramp, (3) hydrophobic powder bed, and (4) electromagnet location. The electromagnet is positioned at the back, out of view in these photos. All scale bars are 30 mm.

powder bed of UHDPE. Nickel LMs were made using a superhydrophobic surface (see above) to pre-form the droplet sphere, before rolling in an appropriate powder. A magnified view of both a Ni/UHDPE hybrid LM and a nickel LM can be seen in figure 4.

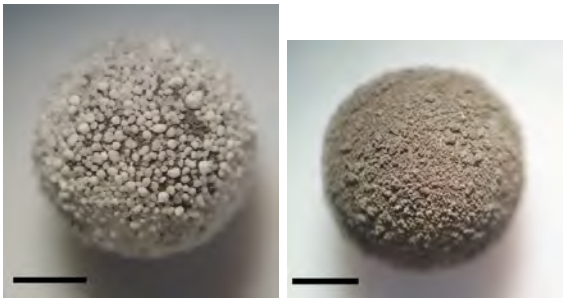

(a) (b)

Figure 4: Magnified photographs of (a) a Ni/UHDPE LM, nickel can clearly be seen between the UHDPE particles; and (b) a pure nickel LM. Scale bars are 1.0 mm.

From the data shown in table 1, it can be seen that both the nickel and UHDPE LMs have slower evaporation rates than a pure water droplet. This is expected, as the solid particles on the surface of the liquid form an (incomplete) barrier to evaporation. It also supports previous studies [39]. Experiments also indicated that pure UHDPE LMs evaporate at a comparable rate to pure nickel LMs. This is due to a balancing act between the short narrow pores of the nickel LM, the long wide channels of the UHDPE LM, and the much larger contact angle of UHDPE compared to nickel [40, 41]. The larger grain size of the UHDPE creates longer channels for water vapour to traverse. This results in a smaller water vapour concentration gradient.

It is noteworthy that the new hybrid LM offers the best protection, with the lowest rate of evaporation. It is suggested that this is due to differences

Table 1: Comparison of the evaporation rates (standard deviations in brackets) for 10 µl LMs and an uncoated water droplet.

LM Coating	**Initial Evaporation Rate** $\mathrm{mg\,min^{-1}}$
(Water Droplet)	0.13 (0.01)
Ni	0.12 (0.01)
UHDPE	0.12 (0.02)
Ni/UHDPE	0.10 (0.01)

in the nickel and UHDPE particle sizes. This difference is clearly visible in the magnified photograph shown in figure 4(a). The larger UHDPE particles offer good resistance to evaporation, due to their thickness. However, this also leads to large gaps between the particles, due to poor packing. This problem is alleviated by the nickel particles filling the available space. The use of two differently sized spheres for 3D spherical packing is well documented [42, 43], and has been shown to increase the maximum perfect packing density beyond the 0.74 limit of a single-sized 3D sphere packing, to 0.93 for an ideal binary system [44]. In this instance, due to the multilayer nature of the LM coating [13], it is more appropriate to relate to 3D sphere packing than 2D circle packing.

3.2. Liquid Marble Collisions

If the gate timings are not accurate, then the LMs will continue on their separate paths and shall not collide. If the timings are accurate, and it is taken that the two LMs are identical, then there are three possible outcomes of the collision. Firstly, that the LMs collide with some elastic property, and then continue on two distinct and new paths. Secondly, that the LMs collide with no elastic property, then continue vertically as two adjacent, but distinct, LMs. Thirdly, that on collision the LMs coalesce into a larger single LM with zero lateral velocity, which continues vertically down.

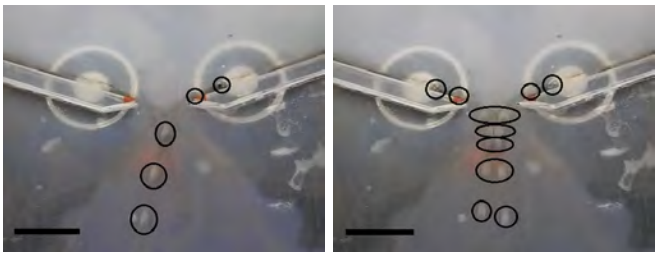

(a) (b)

Figure 5: Overlaid still frames of (a) a single LM, with frames at 0 ms, 142 ms, 209 ms, 242 ms and 267 ms; and (b) two colliding LMs, with frames at 0 ms, 125 ms, 200 ms, 217 ms, 225 ms, 250 ms and 275 ms. Both scale bars are 20 mm.

Video snapshots showing both a single uninterrupted and a colliding pair of LMs, can be seen in figure 5. The time between the LMs leaving the ramp, colliding and being visually separated again, is 75 ms. This represents an upper limit on LM collision-based computing time for a 1-bit calculation. Analysis from ten collisions show only a slight deviation in the collision exit trajectory. By taking a vertical line from the centre of the collision as the reference line, the exit trajectories for the LMs are $-5.3 \pm 1.5°$ and $+5.5 \pm 1.1°$.

Our experiments demonstrate that LMs collide in an elastic manner. This is unsurprising, due to their previously reported soft-shell and compressible nature [1, 45]. It also supports the previously published, linear, non-coalescing collision of LMs [45]. The elastic properties and compressible nature of LMs has been discussed elsewhere in a recent review [46]. By monitoring the collisions at 120 fps, it was observed that LMs behave like two soft balls, acting in a manner described in the Soft Sphere Model (SSM), known as a Margolus gate [34]. A video of a typical collision can be seen in the supporting information. The important distinction between the SSM and the better known Billiard Ball Model (BBM) [25], is the exit points of the colliding particles compared to the non-colliding particles. In the BBM, the particles are taken to be hard spheres, which instantly rebound off each other — leading to the **AB** paths being outside the corresponding $\bar{\mathbf{A}}\mathbf{B}$ and $\mathbf{A}\bar{\mathbf{B}}$ paths. In contrast, the SSM accounts for the finite and appreciable amount of time required for real-world soft spheres to rebound. The result is that the AB paths move to lie inside the unchanged $\bar{\mathbf{A}}\mathbf{B}$ and $\mathbf{A}\bar{\mathbf{B}}$ paths. The BBM and SSM pathways can be seen in figures 6(a) and 6(b), respectively.

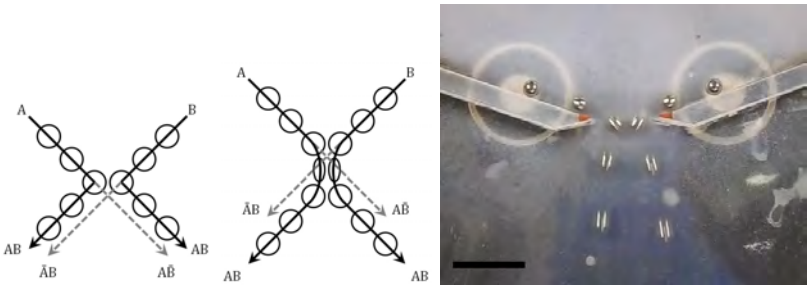

(a) (b) (c)

Figure 6: Showing the colliding and non-colliding routes for (a) BBM and (b) SSM pathways. (c) A collision of steel balls, following BBM under gravity (cf. SSM LMs above). Frame times are 0 ms, 175 ms, 242 ms, 284 ms and 325 ms. Scale bar is 20 mm.

It was possible to break the SSM analogy by increasing the speed of the LMs. The speed of the LMs was calculated by measuring the distance travelled by the LM in a certain number of frames, and knowing the recording frames per second. When the collision happens at $0.21\,\mathrm{m\,s^{-1}}$, the LMs bounce elastically following SSM paths. However, when the speed of collision is increased to $0.29\,\mathrm{m\,s^{-1}}$, the two LMs coalesce. This can be seen in the video snapshots in figure 7. It

should be noted that the previously mentioned LM computing time is reduced to 50 ms, when the LMs are permitted to coalesce. This is measured from when the LMs leave the ramp, to when they are fully coalesced. The time is saved by not requiring the LMs to separate.

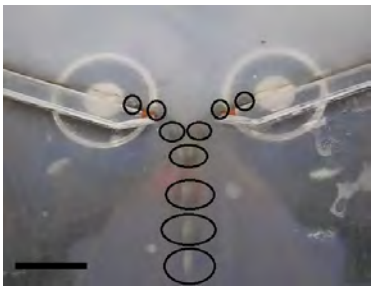

Figure 7: Overlaid still frames showing the coalescence of two colliding LMs. Frames shown at 0 ms, 117 ms, 159 ms, 184 ms, 209 ms, 234 ms and 250 ms. Scale bar is 20 mm.

Growth by coalescence of LMs is a commonly observed effect [47]. For a computing device, the physical nature of the input and output signals should be exactly the same. When two LMs coalesce, the output mass is double a single input mass. Consequently, if colliding LMs at this higher speed, a splitting device would be required to reduce the mass of the output LM. The facile splitting of a LM using a superhydrophobic treated scalpel has previously been reported [48].

By analysing the output paths of the LM collider, it becomes apparent that the gate could be modified to act as a 1-bit half-adder, with the possible outcomes demonstrated in figure 8. When a single LM traverses the system from the **A** or **B** channel, it finishes at the left or right extremes, the $\mathbf{A}\bar{\mathbf{B}}$ or $\bar{\mathbf{A}}\mathbf{B}$ path, respectively. Once the exit pathways are combined, this is analogous to the sum output on a half-adder. An initial trial confirming feasibility of this is shown in figure 8(a), where a single LM enters from the right channel, crosses the gap, and is reflected to exit on the right side.

When two synchronised LMs pass through the collider, they either rebound or coalesce, according to their velocity at impact. If the LMs coalesce, then the new LM travels straight down the only **AB** path, which can be considered to be the carry output. Alternatively if the LMs rebound, as in the SSM, then there are two **AB** paths. One of these paths is then considered to be the carry output, and the other is discarded (the choice between the two **AB** paths is arbitrary in this case). As stated above, there are approximately 10° of departure between the two **AB** paths, making separation facile.

3.3. One-Bit Full-Adder Proposed

By using this design (complete with magnetic timing control) and an intuitive XOR gate, we can adapt the model of the one-bit full-adder proposed originally for Belousov-Zhabotinsky medium [49]. The XOR gate can be replaced

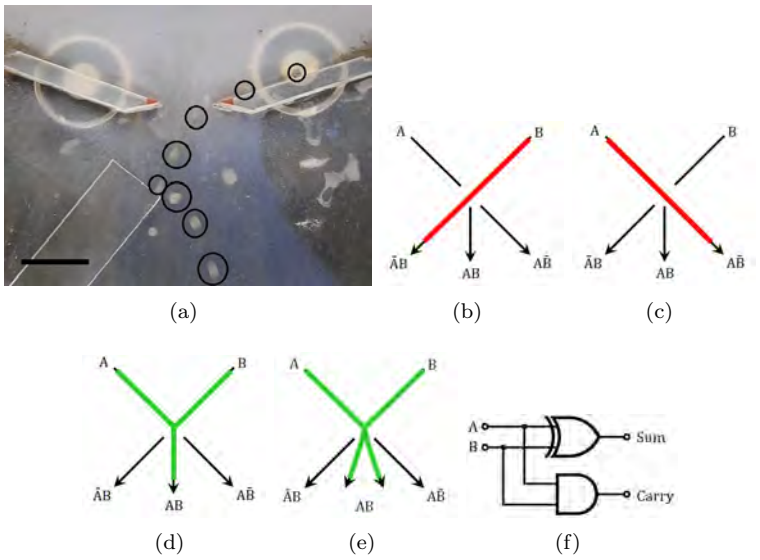

Figure 8: (a) Overlaid frames showing the successful reflection of a LM, frames are timed at 0 ms, 234 ms, 334 ms, 375 ms, 400 ms, 434 ms, 476 ms and 517 ms. Scale bar is 20 mm. (b) & (c) The outcomes of a single unreflected LM passing through the adder. (d) The outcome of the adder when two LMs collide and coalesce. (e) The outcome of the adder when two LMs collide according to the SSM. (f) The electronic representation of a 1-bit half-adder.

with an OR gate without loss of logic, as there is no situation where two LMs will arrive simultaneously. The design schematic can be seen in figure 9. There are two sets of electromagnets, which cycle on-off in pairs; first EM1 releases, then shortly after EM2 releases. This maintains synchronisation between LMs across the two collision gates. The signal delays (indicated in figures 9 and 10 by wavy lines) are useful for helping timing control for any future additional cascades. These can be implemented using channel curves, reflectors, or with EMs. The EM's delay could be controlled using capacitance. Additionally, the $\mathbf{C_{in}}$ channel could be released simultaneously with the **A** and **B** channel, using signal delay to ensure collision.

For this design iteration, we have used channels for the passage of LMs. This is a deviation from pure collision-based computing, where free-space is used as momentary 'wires' on an ad hoc basis. However, in this case, we believe the use of channels to be an important intermediate step towards this goal.

For the example operations visualised in figure 10, if a LM travels down the **A** and **B** channel, then they will collide and travel straight to the carry output. If a LM travels down the **B** and $\mathbf{C_{in}}$ paths, then the **B** LM crosses the first gate, before colliding with the $\mathbf{C_{in}}$ LM and travelling straight down to join the carry output. If a single LM travels down the **B** path, it will cross the first and second gate, finishing on the sum output. If a LM travels down the **A**, **B** and $\mathbf{C_{in}}$ paths, then **A** and **B** will collide at the first gate and go straight to

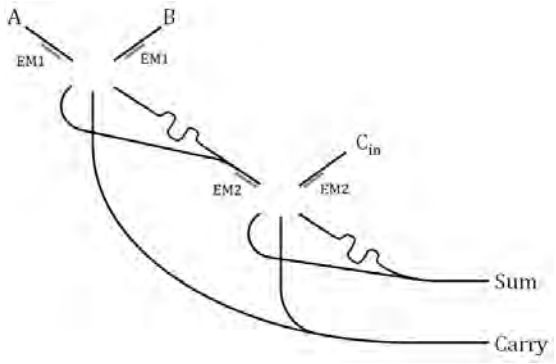

Figure 9: The general design schematic for a 1-bit full-adder, operated using liquid marbles.

the carry output, whilst the $\mathbf{C_{in}}$ LM will cross its gate and finish on the sum output.

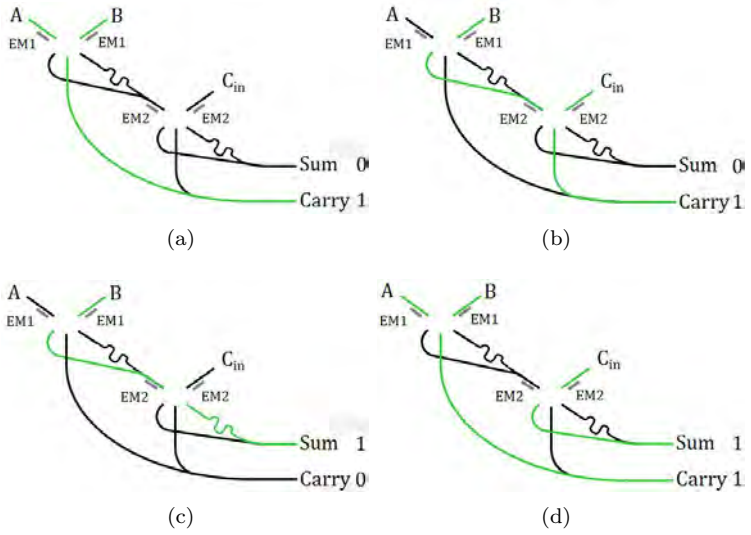

Figure 10: Example operations of the 1-bit full-adder to sum (a) $1+1+0=10$, (b) $0+1+1=10$, (c) $0+1+0=01$, and (d) $1+1+1=11$.

Based on the observations of our collision gate, we note that such a full-adder could be implemented with dimensions of approximately 15 cm × 15 cm, using LMs with a volume of approximately 10 µl, and a LM pre-collision run length of 2 cm. This gate could then be cascaded as required to produce an n-bit full-adder. Signal timing across multiple cascading gates would be controlled using multiple stage EMs. Empirical testing has shown that reliable and manipulable LMs can be formed down to 1.0 µl, meaning that the device could then be scaled

down appropriately. Using a single set of syringes, the automatic marble maker can up to eight LMs per needle per second. At this speed, synchronisation of the electromagnets becomes crucial. Initial investigations into the collision lifetime of the LM are promising, with six 10.0 µl LMs confined to a 2.5 cm × 2.5 cm space on an orbital shaker at 100 rpm (covered to minimise evaporation), showing no signs of wear after three hours.

4. Conclusions

In summary, this demonstration of a collision interaction gate represents the first computing device operated by LMs. A new automatic technique for the easy and reproducible synthesis of LMs enhances the reliability of gate operations. The novel electromagnetic synchronisation of the LM collisions was made possible by the development of a new magnetic hybrid LM, with a coating composed of nickel and UHDPE, used in conjunction with electromagnets for breaking, holding, and synchronised release of the LMs. This collision gate would operate as a 1-bit half-adder, once the sum outputs are combined. A design schematic for a 1-bit full-adder was proposed.

The use of LMs for collision-based computation has many advantages (additional degrees of freedom) over previous approaches. Due to their nature, it is possible to carry cargo in the LMs, which adds an additional dimension to the calculations. It is also possible to initiate chemical reactions within marbles by their coalescence [12]. By varying the diameters of the LMs, different sizes can represent different values, and will have different relative trajectories — removing the limitations of a binary system. Use of a magnet can remove the coating from magnetic marbles, which (if done on a superhydrophobic surface) can roll freely down a slope as droplets, before being reformed using a different coating. Compared to droplet computing [35, 50], only a tiny portion of the circuit needs to be treated hydrophobic, making larger and more complicated circuits easier and cheaper to construct. These points, combined with LM's ability to be easily merged, levitated [12], divided [48], opened/closed [51], and easily propelled by a variety of methods make LMs a fascinating and potentially prosperous addition to the unconventional computing family.

We envision the continued development of LM arithmetic circuits, and are currently working on producing working models of cascading standard gates.

Acknowledgements

This research was supported by the EPSRC with grant EP/P016677/1 "Computing with Liquid Marbles". The authors thank Dr Richard Mayne for his help with microscope imaging.

Supporting Information

Video footage of the liquid marble collisions is available in the supporting information.

References

[1] P. Aussillous, D. Quéré, Liquid marbles, Nature 411 (6840) (2001) 924–927. doi:10.1038/35082026.
URL http://www.nature.com/doifinder/10.1038/35082026

[2] F. Sarvi, K. Jain, T. Arbatan, P. J. Verma, K. Hourigan, M. C. Thompson, W. Shen, P. P. Y. Chan, Cardiogenesis of Embryonic Stem Cells with Liquid Marble Micro-Bioreactor, Adv. Healthc. Mater. 4 (1) (2015) 77–86. doi:10.1002/adhm.201400138.
URL http://doi.wiley.com/10.1002/adhm.201400138

[3] S. Ledda, A. Idda, J. Kelly, F. Ariu, L. Bogliolo, D. Bebbere, A novel technique for in vitro maturation of sheep oocytes in a liquid marble microbioreactor, J. Assist. Reprod. Genet. 33 (4) (2016) 513–518. doi:10.1007/s10815-016-0666-8.
URL http://link.springer.com/10.1007/s10815-016-0666-8

[4] S. Fujii, S. Takeuchi, M. Edahiro, S. Yoshimi, A. Kogure, Y. Tarui, M. Kasahara, Y. Yasui, Y. Nakamura, Pressure-sensitive Adhesive Liquid Marble: Fabrication and Characterization of Structure and Adhesive Property, J. Japan Soc. Powder Powder Metall. 64 (3) (2017) 121–125. doi:10.2497/jjspm.64.121.
URL https://www.jstage.jst.go.jp/article/jjspm/64/3/64{_}121/{_}article/-char/ja/

[5] J. Tian, T. Arbatan, X. Li, W. Shen, Porous liquid marble shell offers possibilities for gas detection and gas reactions, Chem. Eng. J. 165 (1) (2010) 347–353. doi:10.1016/j.cej.2010.06.036.
URL http://linkinghub.elsevier.com/retrieve/pii/S1385894710005693

[6] M. Paven, H. Mayama, T. Sekido, H.-J. Butt, Y. Nakamura, S. Fujii, Light-Driven Delivery and Release of Materials Using Liquid Marbles, Adv. Funct. Mater. 26 (19) (2016) 3199–3206. doi:10.1002/adfm.201600034.
URL http://doi.wiley.com/10.1002/adfm.201600034

[7] W. Wei, R. Lu, W. Ye, J. Sun, Y. Zhu, J. Luo, X. Liu, Liquid Marbles Stabilized by Fluorine-Bearing Cyclomatrix Polyphosphazene Particles and Their Application as High-Efficiency Miniature Reactors, Langmuir 32 (7) (2016) 1707–1715. doi:10.1021/acs.langmuir.5b04697.
URL http://pubs.acs.org/doi/abs/10.1021/acs.langmuir.5b04697

[8] E. Bormashenko, R. Pogreb, R. Balter, H. Aharoni, D. Aurbach, V. Strelnikov, Liquid marbles containing petroleum and their properties, Pet. Sci. 12 (2) (2015) 340–344. doi:10.1007/s12182-015-0016-y.
URL http://link.springer.com/10.1007/s12182-015-0016-y

[9] M. K. Khaw, C. H. Ooi, F. Mohd-Yasin, R. Vadivelu, J. S. John, N.-T. Nguyen, Digital microfluidics with a magnetically actuated floating liquid marble, Lab Chip 16 (12) (2016) 2211–2218. doi:10.1039/C6LC00378H.
URL http://xlink.rsc.org/?DOI=C6LC00378H

[10] P. Aussillous, D. Quéré, Properties of liquid marbles, Proc. R. Soc. A Math. Phys. Eng. Sci. 462 (2067) (2006) 973–999. doi:10.1098/rspa.2005.1581.
URL http://rspa.royalsocietypublishing.org/cgi/doi/10.1098/rspa.2005.1581

[11] C. H. Ooi, A. van Nguyen, G. M. Evans, O. Gendelman, E. Bormashenko, N.-T. Nguyen, A floating self-propelling liquid marble containing aqueous ethanol solutions, RSC Adv. 5 (122) (2015) 101006–101012. doi:10.1039/C5RA23946J.
URL http://xlink.rsc.org/?DOI=C5RA23946J

[12] Z. Chen, D. Zang, L. Zhao, M. Qu, X. Li, X. Li, L. Li, X. Geng, Liquid Marble Coalescence and Triggered Microreaction Driven by Acoustic Levitation, Langmuir 33 (25) (2017) 6232–6239. doi:10.1021/acs.langmuir.7b00347.
URL http://pubs.acs.org/doi/abs/10.1021/acs.langmuir.7b00347

[13] D. Dupin, S. P. Armes, S. Fujii, Stimulus-responsive liquid marbles, J. Am. Chem. Soc. 131 (15) (2009) 5386–5387.

[14] S. Fujii, S. Kameyama, S. P. Armes, D. Dupin, M. Suzaki, Y. Nakamura, pH-responsive liquid marbles stabilized with poly(2-vinylpyridine) particles, Soft Matter 6 (3) (2010) 635–640. doi:10.1039/B914997J.
URL http://xlink.rsc.org/?DOI=B914997J

[15] B. Peter, "and" gate, US Patent 3,191,611 (June 1965).

[16] C. A. Belsterling, Fluidic systems design, John Wiley & Sons, 1971.

[17] A. Adamatzky, Collision-based computing in Belousov–Zhabotinsky medium, Chaos Solitons Fract. 21 (5) (2004) 1259–1264.

[18] A. Adamatzky, B. de Lacy Costello, Binary collisions between wave-fragments in a sub-excitable Belousov–Zhabotinsky medium, Chaos Solitons Fract. 34 (2) (2007) 307–315.

[19] R. Toth, C. Stone, B. d. L. Costello, A. Adamatzky, L. Bull, Simple Collision-Based Chemical Logic Gates with Adaptive Computing, in: Theor. Technol. Adv. Nanotechnol. Mol. Comput., IGI Global, 2010, pp. 162–175. doi:10.4018/978-1-60960-186-7.ch011.
URL http://services.igi-global.com/resolvedoi/resolve.aspx?doi=10.4018/978-1-60960-186-7.ch011

[20] A. Adamatzky, B. De Lacy Costello, L. Bull, J. Holley, Towards arithmetic circuits in sub-excitable chemical media, Isr. J. Chem. 51 (1) (2011) 56–66.

[21] R. Mayne, A. Adamatzky, On the Computing Potential of Intracellular Vesicles, PLoS One 10 (10) (2015) e0139617. doi:10.1371/journal.pone.0139617.
URL http://dx.plos.org/10.1371/journal.pone.0139617

[22] Y.-P. Gunji, Y. Nishiyama, A. Adamatzky, T. E. Simos, G. Psihoyios, C. Tsitouras, Z. Anastassi, Robust soldier crab ball gate, Complex Syst. 20 (2) (2011) 93.

[23] E. R. Berlekamp, J. H. Conway, R. K. Guy, Winning Ways, for Your Mathematical Plays: Games in particular, Vol. 2, Academic Press, 1982.

[24] A. Adamatzky, B. de Lacy Costello, L. Bull, On polymorphic logical gates in subexcitable chemical medium, Int. J. Bifurc. Chaos 21 (07) (2011) 1977–1986.

[25] E. Fredkin, T. Toffoli, Conservative logic, in: Collision-based computing, Springer, 2002, pp. 47–81.

[26] T. Toffoli, Reversible computing, in: International Colloquium on Automata, Languages, and Programming, Springer, 1980, pp. 632–644.

[27] A. De Vos, Reversible computing: fundamentals, quantum computing, and applications, John Wiley & Sons, 2011.

[28] C. H. Bennett, Notes on the history of reversible computation, IBM J. Res. Dev. 32 (1) (1988) 16–23.

[29] G. P. Berman, G. D. Doolen, D. D. Holm, V. I. Tsifrinovich, Quantum computer on a class of one-dimensional Ising systems, Phys. Lett. A 193 (5-6) (1994) 444–450.

[30] A. Barenco, C. H. Bennett, R. Cleve, D. P. DiVincenzo, N. Margolus, P. Shor, T. Sleator, J. A. Smolin, H. Weinfurter, Elementary gates for quantum computation, Phys. Rev. A 52 (5) (1995) 3457.

[31] J. A. Smolin, D. P. DiVincenzo, Five two-bit quantum gates are sufficient to implement the quantum Fredkin gate, Phys. Rev. A 53 (4) (1996) 2855.

[32] S.-B. Zheng, Implementation of Toffoli gates with a single asymmetric Heisenberg x y interaction, Phy. Rev. A 87 (4) (2013) 042318.

[33] N. Kostinski, M. P. Fok, P. R. Prucnal, Experimental demonstration of an all-optical fiber-based Fredkin gate, Opt. Lett. 34 (18) (2009) 2766–2768.

[34] N. Margolus, Universal cellular automata based on the collisions of soft spheres, in: A. Adamatzky (Ed.), Collision-based computing, Springer, 2002, pp. 107–134.

[35] H. Mertaniemi, R. Forchheimer, O. Ikkala, R. H. A. Ras, Rebounding Droplet-Droplet Collisions on Superhydrophobic Surfaces: from the Phenomenon to Droplet Logic, Adv. Mater. 24 (42) (2012) 5738–5743. doi:10.1002/adma.201202980.
URL http://doi.wiley.com/10.1002/adma.201202980

[36] N. Eshtiaghi, J. S. Liu, W. Shen, K. P. Hapgood, Liquid marble formation: Spreading coefficients or kinetic energy?, Powder Technol. 196 (2) (2009) 126–132. doi:10.1016/j.powtec.2009.07.002.
URL http://linkinghub.elsevier.com/retrieve/pii/S0032591009004100

[37] J. Tian, T. Arbatan, X. Li, W. Shen, Liquid marble for gas sensing, Chem. Commun. 46 (26) (2010) 4734. doi:10.1039/c001317j.
URL http://xlink.rsc.org/?DOI=c001317j

[38] J. Tian, N. Fu, X. D. Chen, W. Shen, Respirable liquid marble for the cultivation of microorganisms, Colloids Surf. B 106 (2013) 187–190. doi:10.1016/j.colsurfb.2013.01.016.
URL http://linkinghub.elsevier.com/retrieve/pii/S0927776513000386

[39] M. Dandan, H. Y. Erbil, Evaporation Rate of Graphite Liquid Marbles: Comparison with Water Droplets, Langmuir 25 (14) (2009) 8362–8367. doi:10.1021/la900729d.
URL http://pubs.acs.org/doi/abs/10.1021/la900729d

[40] D. J. Trevoy, H. Johnson, The Water Wettability of Metal Surfaces, J. Phys. Chem. 62 (7) (1958) 833–837. doi:10.1021/j150565a016.
URL http://pubs.acs.org/doi/abs/10.1021/j150565a016

[41] L. Ammosova, Y. Jiang, M. Suvanto, T. A. Pakkanen, Selective three-dimensional hydrophilization of microstructured polymer surfaces through confined photocatalytic oxidation, Appl. Surf. Sci. 329 (2015) 58–64. doi:10.1016/j.apsusc.2014.12.147.
URL http://linkinghub.elsevier.com/retrieve/pii/S0169433214028736

[42] S. Yamada, J. Kanno, M. Miyauchi, Multi-sized Sphere Packing in Containers: Optimization Formula for Obtaining the Highest Density with Two Different Sized Spheres, Inf. Media Technol. 6 (2) (2011) 493–500. doi:10.11185/imt.6.493.
URL https://www.jstage.jst.go.jp/article/imt/6/2/6{_}2{_}493/{_}article

[43] H. Y. Sohn, C. Moreland, The effect of particle size distribution on packing density, Can. J. Chem. Eng. 46 (3) (1968) 162–167. doi:10.1002/cjce.5450460305.
URL http://doi.wiley.com/10.1002/cjce.5450460305

[44] A. R. Kansal, S. Torquato, F. H. Stillinger, Computer generation of dense polydisperse sphere packings, J. Chem. Phys. 117 (18) (2002) 8212–8218. doi:10.1063/1.1511510.
URL http://aip.scitation.org/doi/10.1063/1.1511510

[45] E. Bormashenko, R. Pogreb, R. Balter, H. Aharoni, Y. Bormashenko, R. Grynyov, L. Mashkevych, D. Aurbach, O. Gendelman, Elastic properties of liquid marbles, Colloid Polym. Sci. 293 (8) (2015) 2157–2164. doi:10.1007/s00396-015-3627-3.
URL http://link.springer.com/10.1007/s00396-015-3627-3

[46] E. Bormashenko, Liquid Marbles, Elastic Nonstick Droplets: From Minireactors to Self-Propulsion, Langmuir 33 (3) (2017) 663–669. doi:10.1021/acs.langmuir.6b03231.
URL http://pubs.acs.org/doi/abs/10.1021/acs.langmuir.6b03231

[47] P. S. Bhosale, M. V. Panchagnula, Sweating Liquid Micro-Marbles: Dropwise Condensation on Hydrophobic Nanoparticulate Materials, Langmuir 28 (42) (2012) 14860–14866. doi:10.1021/la303133y.
URL http://pubs.acs.org/doi/abs/10.1021/la303133y

[48] E. Bormashenko, Y. Bormashenko, Non-Stick Droplet Surgery with a Superhydrophobic Scalpel, Langmuir 27 (7) (2011) 3266–3270. doi:10.1021/la200258u.
URL http://pubs.acs.org/doi/abs/10.1021/la200258u

[49] A. Adamatzky, Binary full adder, made of fusion gates, in a subexcitable Belousov-Zhabotinsky system, Phys. Rev. E 92 (3) (2015) 032811.

[50] G. Katsikis, J. S. Cybulski, M. Prakash, Synchronous universal droplet logic and control, Nat. Phys. 11 (7) (2015) 588–596. doi:10.1038/nphys3341.
URL http://www.nature.com/doifinder/10.1038/nphys3341

[51] Y. Zhao, J. Fang, H. Wang, X. Wang, T. Lin, Magnetic Liquid Marbles: Manipulation of Liquid Droplets Using Highly Hydrophobic Fe_3O_4 Nanoparticles, Adv. Mater. 22 (6) (2010) 707–710. doi:10.1002/adma.200902512.
URL http://doi.wiley.com/10.1002/adma.200902512